Modeling Feasible Locomotion of Nanobots for Cancer Detection and Treatment

NOBLE HARASHA, Massachusetts Institute of Technology, USA
CRISTINA GAVA, King's College London, UK
NANCY LYNCH, Massachusetts Institute of Technology, USA
CLAUDIA CONTINI, Imperial College London, UK
FREDERIK MALLMANN-TRENN, King's College London, UK

Deploying nanoscopic particles and robots in the human body promises increasingly selective drug delivery with fewer side effects. We consider the problem of a homogeneous swarm of nanobots locating a singular cancerous region and treating it by releasing some onboard payload of drugs once at the site. At nanoscale, the computation, communication, sensing, and locomotion capabilities of individual agents are extremely limited, noisy, and/or nonexistent. We present a general model to formally describe the individual and collective behaviour of agents in a colloidal environment, such as the bloodstream, for the problem of cancer detection and treatment by nanobots. This includes a feasible and precise model of agent locomotion, which is inspired by actual nanoscopic vesicles which, when in the presence of an external chemical gradient, tend towards areas of higher concentration by means of self-propulsion. The delivered payloads have a dual purpose of treating the cancer, as well as diffusing throughout the space to form a chemical gradient which other agents can sense and noisily ascend. We present simulation results to analyze the behavior of individual agents under our locomotion model and to investigate the efficacy of this collectively amplified chemical signal in helping the larger swarm efficiently locate the cancer site.

1 INTRODUCTION

Nanobots possess great potential in many medical applications as their scale allows for: maneuverability within otherwise unreachable regions of the body, the deployment of swarms containing significantly high numbers of individual agents, and general precision. We consider the dual problem of cancer detection and treatment in the context of nanomedicine, whose use holds significant promise. Nanoparticles, or nanobots, are being studied and engineered to move within the human body and target sites, such as, cancer sites, in order to offer treatment by releasing cancer drugs. This approach offers a drug delivery solution which is more selective, and thus less toxic to extraneous regions, especially in comparison to existing methods of treatments such as chemotherapy. This promising approach, however, faces a number of challenges: control on the behaviour of these robots is often limited, if not absent, for example, due to the very small size of these agents. If externally controlled movement is to be included, it then comes at the cost of having larger-scale robots.

We therefore investigate the interesting and crucial challenge of nanobots' ability to distributively and autonomously find a cancerous site, and subsequently treat it. In this work, we consider this process to be stochastic in nature, with nanobots performing some of biased random walk, influenced by the physics of the environment they navigate through.

In Section 1.1 we give an overview of the current literature related to this problem. Section 2 formally describes the general model we propose, with a particular focus on the model of agent locomotion which is inspired by actual nanoparticles. We then present simulation results for the 2-dimensional setting in Section 3 and conclude the work with a brief discussion and suggestions for future work.

1.1 Related Work

At the end of the 20^{th} century, the first ideas on nanotechnology and its potential applications in medicine emerged and laid the groundwork for the development of the field of nanomedicine. The works in [3] and [5] present one of the first introductions to the concept of nanotechnology and the potential gains of its use for medical purposes, including drug delivery, diagnostics and tissue engineering. In this work, we study the application of nanoparticles to drug delivery for cancer treatment, as explored in [1, 11, 15]. The main motivation behind the use of nanoparticles is the reduction of systemic side effects in favour of a treatment with the same level of efficacy, if not higher.

Extensive work looks at the diffusion and motion of nanoparticles in the bloodstream from a *centralised* perspective [13], often employing external magnetic fields for control of agent locomotion [8, 14]. Authors in [7], instead, focused on the *passive*

Authors' addresses: Noble Harasha, Massachusetts Institute of Technology, 77 Massachusetts Ave, Cambridge, MA, USA, nharasha@mit.edu; Cristina Gava, King's College London, Strand, London, UK, cristina.gava@kcl.ac.uk; Nancy Lynch, Massachusetts Institute of Technology, 77 Massachusetts Ave, Cambridge, MA, USA, lynch@csail.mit.edu; Claudia Contini, Imperial College London, London, UK, c.contini@imperial.ac.uk; Frederik Mallmann-Trenn, King's College London, Strand, London, UK, frederik.mallmann-trenn@kcl.ac.uk.

displacement of nanobots in the human body, where agents have zero locomotion capabilities and only change position by following the flow of the circulatory system. Our study, however, follows a group of works where nanobots are thought to be able to move *autonomously* and *distributively* in a space, via performing some sort of random walk. We take inspiration from a series of studies, such as [2, 4, 12], where nanoparticles are seen as possibly performing a Levy walk and where theoretical arguments for the validity of a Levy walk are presented.

In many studies, such as [2], particles move through the mechanism of so-called *chemotaxis*, described as the movement of organisms in response to a chemical stimulus, particularly, a chemical gradient. Many of these studies consider a *colloidal solution* – a mixture where one substance, made of microscopic, insoluble particles, is dispersed in another substance, which is usually termed the *medium* of the solution – and analyse the movement of these particles. Among these works, deeply relevant are the studies in [6], [9] and [10]. In [9], authors analyse the movement of nanoparticles in a colloidal solution where the walk being performed is detailed, and includes the characterisation of a drift velocity and a rotational velocity. Both [9] and [6], however, look at self propulsion of nanoparticles, where the medium in which they are suspended does not present any particular gradient to follow. In [10], instead, authors present an in-vitro empirical analysis of nanoparticles movement following the concentration gradient of a chemical dissolved in the colloidal solution. The authors show how it is precisely the presence of this gradient that favours a precise type of walk from these particles, characterised by long strides towards a higher chemical concentration, interspersed with random self re-orientation. We build on the empirical results in [10] to create a mathematical model able to rigorously characterise the movement of these particles.

2 MODEL

We present a continuous space, discrete time general model for the problem of cancer detection and treatment by nanobots in the human body, outlining all environment and agent capabilities assumptions. This includes a precise model for agent locomotion.

2.1 General Model

A set of n identical agents—nanobots—move in a d-dimensional Euclidean Space $\mathbb{R}^d$. Time is discretized. We consider one, single cancer site that is concentrated in a single point in space. The cancer site naturally releases some chemical marker, which agents can sense. This allows agents to detect the presence of a nearby cancer site once they are within 1 unit of distance, with perfect accuracy; we consider them to have "reached the cancer site" at this point. Each agent has a payload of some artificial chemical, which other agents can sense. Once an agent is this unitary distance away from the cancer site, it immediately releases its payload and for all practical purposes effectively ceases to exist in the environment. Firstly, this payload chemical contributes in treating the cancer site. Secondly, the payload chemical diffuses perfectly radially out from the cancer site via instantaneous point-source diffusion (see γ below), forming a global chemical gradient centered at the cancer site. This gradient serves to amplify the signal of a nearby cancer site to other agents still exploring. This second notion will be formalized by the movement model in the next section. No direct interaction/communication occurs between agents. The agents' movement is only a function of their their previous state and the chemical they're currently sensing.

We investigate the agents' ability to distributively and autonomously locate the cancer site and release their payloads (i.e., the treatment). Given individual agents' random/noisy behavior, our goal will be for just 75% of the agents to deliver their marginal treatment. The following quantities are involved in the process.

- The location of the cancer site is indicated with x^* and we assume (w.l.o.g.) without loss of generality, $x^* = \overrightarrow{0}$ (d-dimensional null-vector);
- The location of an agent i (arbitrary index $i \in \mathbb{N}, i \in [0, n-1]$) at time t is $x_i^{(t)} \in \mathbb{R}^d$, and its orientation is the vector $\theta_i^{(t)} \in \mathbb{R}^d$;
- The location of the initial site from which all agents begin is indicated with $x^0 \in \mathbb{R}^d$, i.e., $x_i^{(0)} = x^0 \; \forall i$;
- The number of agents that have released their drug payload up to time t is $y^{(t)} \in \mathbb{N}$, with $y^{(0)} = 0$;

Imagine one agent releases its payload of amount P at the cancer site at time t^*. It will immediately begin diffusing, with the concentration of this individual payload, at location x at time t, being a function of the distance from the cancer site $||x - x^*||_2$ and the time since its release $(t - t^*)$: $\frac{P}{(4\pi D(t-t^*))^{d/2}} \exp\left(-\frac{(||x-x^*||_2)^2}{4D(t-t^*)}\right)$, where D is the diffusion coefficient. We simplify to assume that the diffusion of each agent's payload is independent—i.e., additive.

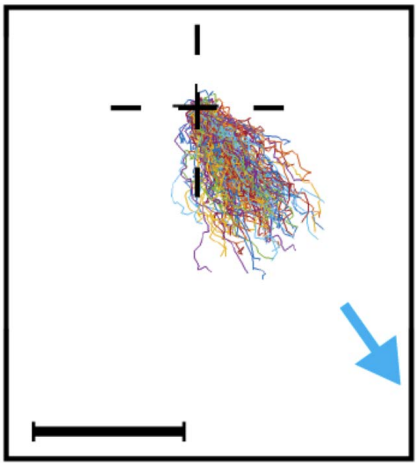

(a) Vesicles in [10]. Chemical gradient increases in the direction of blue arrow. Scale bar is 20μm.

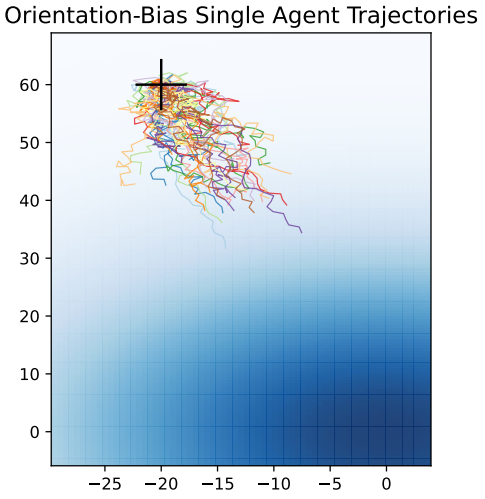

(b) Agents under our model with $b = 0.1$ and a time-constant payload chemical gradient, over 40 runs. Blue gradient represents the payload chemical concentration at a given point.

Fig. 1. Individual agent trajectories (a) in experiment in [10], and (b) in simulation under our model. Black cross indicates agents' initial position.

- Thus, the concentration of the payload chemical at time t at location $x \in \mathbb{R}^d$ is given by

$$\gamma^{(t)}(x) = \frac{P}{(4\pi D)^{d/2}} \sum_{j=1}^{y^{(t)}} \frac{1}{(t - t_j^*)^{d/2}} \exp\left(-\frac{(||x - x^*||_2)^2}{4D(t - t_j^*)}\right)$$

  where t_j^* is the time at which the j'th agent to reach the cancer site released their payload.

2.2 Movement Model

We now describe the update step for the locomotion of an individual agent. All steps are of the same length, but there is a bias of moving towards the cancer site. We call this movement model the *Orientation-Biased Model*.

Consider some agent i. Let $\mu := x^* - x_i^{(t)}$ be the vector pointing from the current agent location to the target location. Let Y be the vector of Gaussian noise, i.e., $Y = [Y_k]_{k\in[d]} \in \mathbb{R}^d$, where each $Y_k \sim \mathcal{N}(0, \sigma^2)$ is set independently, with $\sigma^2 = \left(\gamma^{(t)}\left(x_i^{(t)}\right)\right)^{-b} - \left(\gamma^{(t)}(x^*)\right)^{-b}$ for some constant $b \in \mathbb{R}_{\geq 0}$. Note that the variance is a function of the distance of the agent to cancer site; the larger the distance the larger the noise. Agent i's orientation vector is set as follows.

$$\theta_i^{(t)} = \frac{\mu}{||\mu||_2} + Y$$

That is, there is always a bias to orient towards the cancer site, with a greater bias as the local chemical concentration increases. This bias also increases as b decreases. In fact, as b approaches zero, the movement becomes taking the shortest, straight line path to x^*, and as b approaches infinity, the movement becomes the pure random walk (when $\gamma^{(t)}(x) < 1$). Agent i's position is then updated as follows, taking a step of unitary length in the direction of its orientation vector.

$$x_i^{(t+1)} = x_i^{(t)} + \frac{\theta_i^{(t)}}{||\theta_i^{(t)}||_2}$$

For the scope of this work, we will assume $d = 2$ moving forward, i.e., nanobots are moving in a 2-dimensional space.

2.3 Model Validation

Our model, regarding the locomotion of individual nanobots or agents, is inspired by the actual nanoscopic vesicles presented in [10]. Therefore, it is likely that our model can be implemented to a reasonable extent, and has real-world impact. We now argue that our model resembles the locomotion of nanoparticles in [10] of actual experiment. Our model's artificial payload chemical is the analog of glucose in [10]. Figure 1 shows that agents in our simulation and in the experiment, on average, tend to ascend the global chemical gradient. It is worth noting that the chemical gradient in 1a is linear with respect to the distance to its center and source, while the gradient in 1b is nonlinear as defined by a specific time-constant setting of $\gamma^{(t)}(x) = 0.061 \cdot \exp\left(-\frac{(||x-x^*||_2)^2}{520}\right)$.

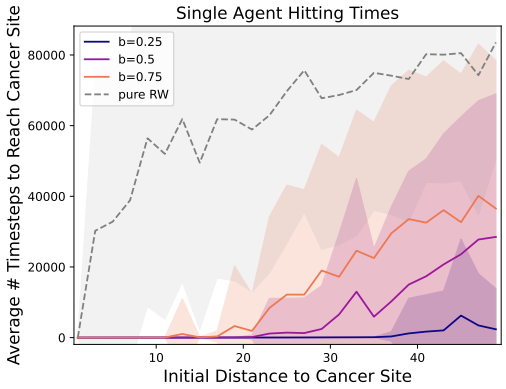

(a) How hitting time scales with the initial distance to the cancer site. Fix chemical gradient, $P = 100$.

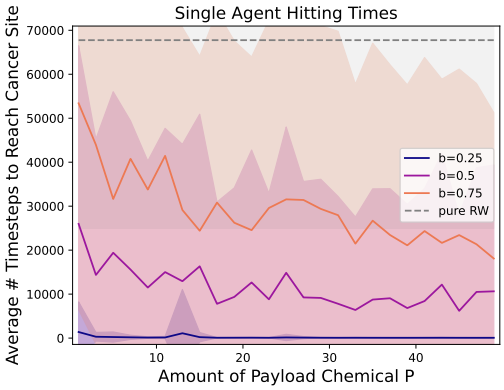

(b) Effect of the magnitude of the payload chemical gradient on hitting time. Fix initial distance to x^* at 30.

Fig. 2. Number of timesteps for a single agent to reach the cancer site (i.e., hitting time) under varying degrees of orientation bias and compared to a pure RW, in the case of a time-constant chemical gradient. Plotted lines are average hitting times over 100 trials, and shaded regions are standard deviations. Hitting times were capped at 100000 timesteps.

The data for [10] could not be obtained, so we're left with a visual comparison with our model's behavior. In a very rough, qualitative manner, we show that our model exhibits behavior that is reasonably similar to the experimental results of [10].

3 SIMULATION RESULTS

In our simulation we only consider the 2-dimensional setting ($d = 2$). We also now impose a boundary on the space such that $\forall x_i^{(t)} = (x, y)$, $-500 \leq x, y \leq 500$. Each time step, an agent's orientation and position vectors are updated until its new position is within the above bounds.

3.1 Single Agent Hitting Times

We first consider the case of a single agent ($n = 1$), simplifying to assume that the global gradient of payload chemical is constant over time. More specifically we let $\gamma^{(t)}(x) = \frac{P}{200\pi}\exp\left(-\frac{(||x-x^*||_2)^2}{200}\right)$. Figure 2 shows the average time it takes one agent following the *Orientation-Biased Model* of locomotion with bias parameter b to reach the cancer site, as well as for one agent following a fully random walk as a baseline of comparison. Recall that lower values of b correspond to agents being more likely to orient and move towards the cancer site (i.e., greater amounts of "orientation-bias").

In Figure 2a, w.l.o.g.—since the chemical gradient is radially symmetric—the agent has initial location $x^0 = (\phi_0, 0)$, where ϕ_0 is the initial distance between the agent and the cancer site x^*. We fix $P = 100$. As ϕ_0 increases, hitting times increase nonlinearly, with this decline in performance worsening with less orientation-bias. However, under these specific environment settings γ, once within a close enough distance (≈ 20) and thus a large enough chemical concentration, agents reach the cancer site very efficiently regardless of the amount of bias. Figure 2b shows the effect of the magnitude of the payload chemical gradient on hitting times. We fix $\phi_0 = 30$. As P increases, hitting time decreases since there is a higher chemical concentration farther out from the cancer site, which the agent senses and consequently orients/moves more favorably in expectation. The effect of P on hitting time is more noticeable under weaker amounts of orientation-bias. As shown in both figures, our movement model significantly outperforms the pure random walk across all settings.

3.2 Collective Amplification of Chemical Gradient

Next, we consider a more dynamic setup involving $n \geq 1$ agents. All agents have the same starting location $x^0 = (25, 0)$. Once an agent reaches the cancer site, it immediately releases its payload which begins to diffuse radially from x^* throughout the environment. Consequently, as defined by γ in our model, the global payload chemical gradient changes over time "passively" as a result of diffusion and "actively" as a result of agents releasing their payloads. Note that the chemical gradient is initially zero everywhere, with agents initially performing purely random walks. As more agents reach the cancer site, they amplify the chemical gradient, thus helping other agents find the cancer site more efficiently. We investigate this collective behavior in simulation.

We define runtime to be the number of timesteps until 75% of the agents have reached the cancer site and released their payload—i.e., delivered their marginal treatment. Figure 3 shows the average runtime with different numbers of agents, for

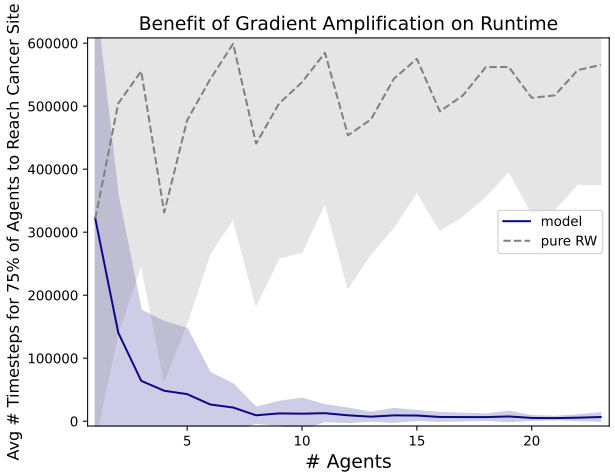

Fig. 3. How runtime scales with the number of agents for both Orientation-Bias and fully RW. Consider the time required for 75% of agents to reach the cancer site and release their payload, where the global payload chemical gradient changes over time as defined by $\gamma^{(t)}(x)$. Fixed parameters include initial distance to cancer of 25, $b = 0.2$, $P = 100$, $D = 0.01$. Plotted lines are average runtimes over 100 trials, and shaded regions are standard deviations. Runtimes were capped at 1000000 timesteps.

our *Orientation-Biased Model* of movement and compared to the case of agents always following pure random walks. We see a significant improvement in runtime as agents increase in number: With more agents releasing their payloads, the global chemical gradient is greater in magnitude resulting in more favorable (biased) agent motion, especially by those that reach the cancer site later on during the given simulation run. In contrast, when agents follow a fully random walk, the average runtime stays relatively constant as the number of agents increases; there is no collective benefit.

With enough agents, the *Orientation-Biased Model* here outperforms the fully random walk by nearly two orders of magnitude. Let T_{PRW} be the runtime associated with the pure random walks, and T_M be our model runtime. For example, with 20 agents, it takes an average of $T_{PRW} = 513123.13$ timesteps for 3/4 of the 20 pure random walks to reach the cancer site, compared to only $T_M = 5186.63$ timesteps for 3/4 of the 20 *Orientation-Biased* (b=0.2) walks to reach; thus, the model performs $98.9 = \frac{T_{PRW}}{T_M}$ times faster than the pure random walk(s). Additionally, as the bias parameter b gets arbitrarily close to zero, $\frac{T_{PRW}}{T_M}$ gets arbitrarily close to $\frac{T_{PRW}}{\phi_0}$, where $\phi_0 = ||x^0 - x^*||_2$ is the initial distance to the cancer site—this ratio can become arbitrarily large as the initial distance to the cancer site increases, since T_{PRW} increases faster as a function of ϕ_0 than ϕ_0 itself.

4 DISCUSSION

We present a formal model of nanbots for cancer detection and treatment, with locomotion capabilities representative of actual nanoparticles. Our results demonstrate that for the *Orientation-Biased Model* of locomotion, agents' movement becomes more favorable as they get closer to the cancer site. The nature of this speedup is a result of the payload chemical concentration function γ, not just the movement model. For the dynamic, multi-agent scenario studied in Section 3.2, we demonstrate a runtime speedup of multiple orders of magnitude with more agents; as more and more agents release their payloads over time, the chemical gradient strengthens, and agents' movement becomes more favorable in general. The second agent to reach the cancer site does so faster in expectation than the first agent because of the amplified chemical gradient, and so on with each subsequent agent. This particular speedup is dramatic enough such that even the *total* time for 3/4 of the walks to reach the cancer site decreases as significantly as it does with more agents. That is, here, agent movement becomes more favorable both when closer to the cancer site *and* as time progresses. Across all settings, our model significantly outperforms the fully random walk.

4.1 Future Work

More thorough validation of the model's practical feasibility via its comparison to actual experiments could be desired. The 3-dimensional setting remains to be investigated. Future work could include studying the effect of different forms of noise on swarm behavior, such as imperfect detection of the cancer site and agent motion impacted by blood flow. Future work could also consider multiple cancer sites, introducing the problem of how to evenly allocate the agents' treatment across all sites even if certain sites are more easily located. This setting could call for more involved strategies such as multiple distinct classes of agents and different injection times. Lastly, it is possible that bounds on the expected hitting time of a single agent can be derived.

REFERENCES

[1] Brigger, I., Dubernet, C., and Couvreur, P. Nanoparticles in cancer therapy and diagnosis. *Advanced drug delivery reviews 64* (2012), 24–36.

[2] Clementi, A., d'Amore, F., Giakkoupis, G., and Natale, E. Search via parallel lévy walks on z2. In *Proceedings of the 2021 ACM Symposium on Principles of Distributed Computing* (2021), pp. 81–91.

[3] Crandall, B. *Nanotechnology: molecular speculations on global abundance*. Mit Press, 1996.

[4] Feola, L., and Trianni, V. Adaptive strategies for team formation in minimalist robot swarms. *IEEE Robotics and Automation Letters 7*, 2 (2022), 4079–4085.

[5] Freitas, R. A. *Nanomedicine, volume I: basic capabilities*, vol. 1. Landes Bioscience Georgetown, TX, 1999.

[6] Golestanian, R., Liverpool, T. B., and Ajdari, A. Propulsion of a molecular machine by asymmetric distribution of reaction products. *Physical review letters 94*, 22 (2005), 220801.

[7] Gómez, J. T., Wendt, R., Kuestner, A., Pitke, K., Stratmann, L., and Dressler, F. Markov model for the flow of nanobots in the human circulatory system. In *Proceedings of the Eight Annual ACM International Conference on Nanoscale Computing and Communication* (2021), pp. 1–7.

[8] Gwisai, T., Mirkhani, N., Christiansen, M. G., Nguyen, T. T., Ling, V., and Schuerle, S. Magnetic torque–driven living microrobots for increased tumor infiltration. *Science Robotics 7*, 71 (2022), eabo0665.

[9] Howse, J. R., Jones, R. A., Ryan, A. J., Gough, T., Vafabakhsh, R., and Golestanian, R. Self-motile colloidal particles: from directed propulsion to random walk. *Physical review letters 99*, 4 (2007), 048102.

[10] Joseph, A., Contini, C., Cecchin, D., Nyberg, S., Ruiz-Perez, L., Gaitzsch, J., Fullstone, G., Tian, X., Azizi, J., Preston, J., et al. Chemotactic synthetic vesicles: Design and applications in blood-brain barrier crossing. *Science Advances 3*, 8 (2017), e1700362.

[11] Kostarelos, K. Nanorobots for medicine: how close are we? *Nanomedicine 5*, 3 (2010), 341–342.

[12] Mallouk, T. E., and Sen, A. Powering nanorobots. *Scientific American 300*, 5 (2009), 72–77.

[13] Martel, S. Nanorobots for microfactories to operations in the human body and robots propelled by bacteria. *Facta universitatis. Series, Mechanics, automatic control and robotics 7*, 1 (2008), 1.

[14] Martel, S., Mohammadi, M., Felfoul, O., Lu, Z., and Pouponneau, P. Flagellated magnetotactic bacteria as controlled mri-trackable propulsion and steering systems for medical nanorobots operating in the human microvasculature. *The International journal of robotics research 28*, 4 (2009), 571–582.

[15] Zhang, D., Gorochowski, T. E., Marucci, L., Lee, H.-T., Gil, B., Li, B., Hauert, S., and Yeatman, E. Advanced medical micro-robotics for early diagnosis and therapeutic interventions. *Frontiers in Robotics and AI 9* (2023), 1086043.